

Magnetic-field-induced Fermi surface reconstruction in $\text{Na}_{0.5}\text{CoO}_2$

L. Balicas,¹ M. Abdel-Jawad,² N. E. Hussey,² F. C. Chou,³ and P. A. Lee⁴

¹*National High Magnetic Field Laboratory, Florida State University, Tallahassee-FL 32306, USA*

²*H. H. Wills Physics Laboratory, University of Bristol, Tyndall Avenue, Bristol BS8 1TL, UK*

³*Center for Materials Science and Engineering, Massachusetts*

Institute of Technology, Cambridge, Massachusetts 02139, USA and

⁴*Department of Physics, Massachusetts Institute of Technology, Cambridge, Massachusetts 02139, USA*

(Dated: November 10, 2018)

We have performed electrical transport measurements at low temperatures and high magnetic fields in $\text{Na}_{0.5}\text{CoO}_2$ single crystals. Shubnikov de Haas oscillations were observed for two frequencies $F_1 \simeq 150$ and $F_2 \simeq 40$ T corresponding respectively to 1 and .25% of the area of the orthorhombic Brillouin zone. These small Fermi surface (FS) pockets indicate that most of the original FS vanishes at the charge ordering (CO) transition. Furthermore, in-plane magnetic fields strongly suppress the CO state. For fields rotating within the conducting planes we observe angular magnetoresistance oscillations (AMRO), whose periodicity changes from two- to six-fold at the transition, suggesting that a reconstructed hexagonal FS emerges at a field of about 40 T.

PACS numbers: 71.18.+y, 72.15.Gd, 71.30.+h

The discovery of superconductivity in hydrated Na_xCoO_2 has stimulated intense interest in this material.[1] The conductive CoO_2 layers can be regarded as an electron-doped correlated $S = 1/2$ triangular network of frustrated Co spins. These electronically active triangular planes of edge sharing CoO_6 octahedra are separated by Na and hydration layers that act not only as spacers, leading to electronic two-dimensionality, but also as charge reservoirs [1, 2]. While many workers have drawn analogy to the high T_c cuprates, the Na_xCoO_2 system is surely of great interest in its own right as one of the few examples of a strongly correlated material with a frustrated lattice where the carrier concentration can be tuned continuously.

The rich phase diagram of the non-hydrated Na_xCoO_2 system as a function of the Na content x [3] reveals a succession of ground states, from a paramagnetic metal at $x = 0.3$ through a charge-ordered (CO) insulator at $x = 1/2$, a “Curie-Weiss metal” for $x \simeq 0.70$, and finally a magnetically ordered state for $x > 0.75$. At $x = 0.5$, detailed electron [4] and neutron [5] diffraction measurements reveal that Na orders in an orthorhombic superstructure that is commensurate with the underlying lattice. Notably, the Na ordering sets in above room temperature though resistivity measurements only show a sharp rise below 53 K, leading to an insulating ground state.[3] The nature of this ground state is unclear. It is presumably induced by the Na ordering, but the low ordering temperature and the sharp onset suggests that it is a nontrivial collective state rather than a band insulator which results from an enlargement of the unit cell due to Na ordering. Photoemission results are not available for the insulating samples, but work on $x = 0.6$ and 0.7 reveals the existence of a large hole-like pocket, with an average radius $k_F \sim 0.65 \pm 0.1 \text{ \AA}^{-1}$, centered around the Γ point.[6] These studies also reveal a very narrow bandwidth $W \sim 100$ meV, confirming the strongly correlated

nature of the cobaltates for $x = 0.6$ and 0.7 .

The key question is what happened to the large hole pocket in the insulating ground state. To gain some insight into this question, we have performed a detailed electrical transport study in $\text{Na}_{0.5}\text{CoO}_2$ at high fields B and low temperatures T . We find that the CO-state observed below $T_{\text{co}} = 53$ K can be suppressed by large in-plane magnetic fields, but not by fields applied along the inter-plane direction. For B rotating within the conductive CoO_2 layers we observe angular magnetoresistance oscillations of essentially two-fold periodicity consistent with the reported orthorhombic crystallographic symmetry of $\text{Na}_{0.5}\text{CoO}_2$ [5]. As B increases (i.e., as the CO-state is suppressed) however, a new 6-fold periodicity emerges indicating the stabilization of a hexagonal FS as reported by the ARPES measurements [6]. This observation suggests on the one hand, that the Na superstructure defines the geometry of the FS at low temperatures, and on the other, that the charge order in the conducting plane is suppressed by high in-plane fields. At low temperatures Shubnikov de Haas oscillations (SdH) of very small frequencies are observed for $B \parallel c$ -axis, indicating that almost the entire FS reported for $x = 0.6$ and 0.7 [6] disappears below T_{co} for $x = 0.5$. Our results strongly indicate that the charge ordering involves the coupling with the Na order and involves the large hole pocket rather than the small pockets near the K points as proposed in Refs. [7, 8, 9].

Single crystals of $\text{Na}_{0.75}\text{CoO}_2$ were grown using the floating-zone technique. By using an electrochemical de-intercalation procedure, samples were produced with a nominal Na concentration $x = 0.5$, as confirmed by Electron Microprobe Analysis. Details of the crystal growth process, the electrochemical de-intercalation technique, and the characterization of the resulting samples are discussed in detail in Ref. [10]. Electrical transport measurements were performed using the standard four-

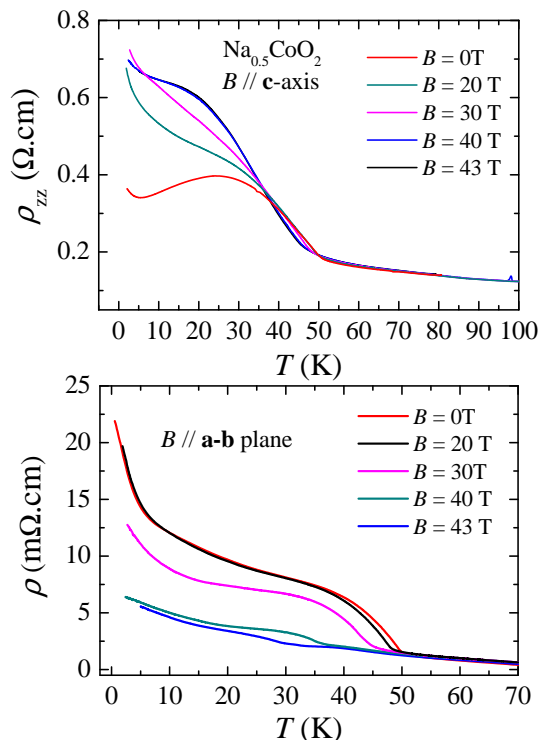


FIG. 1: Upper panel: Inter-plane resistivity ρ_{zz} as a function of temperature T for a $\text{Na}_{0.5}\text{CoO}_2$ single crystal and for several values of the external magnetic field B applied along the inter-plane direction. The sharp increase in resistivity corresponds to a transition towards a charge ordered state. Lower panel: In-plane resistivity ρ as a function of T and for several values of B applied along the conducting planes. Notice the progressive suppression of the CO-state for $B > 20$ T.

terminal technique in a two-axis rotating sample holder inserted in ^3He cryostat. High magnetic fields up to $B = 45$ T were provided by the hybrid magnet at the NHMFL in Tallahassee.

The upper panel of Fig.1 shows the T -dependence of the inter-plane resistivity ρ_{zz} of a $\text{Na}_{0.5}\text{CoO}_2$ single crystal for several values of the external field B applied along the inter-plane c -axis. The abrupt change in slope corresponds to the onset of the charge-ordering at $T_{\text{co}} = 53$ K. B applied along the c -axis has very little effect on T_{co} . Indeed, the absolute value of ρ_{zz} actually increases at lower T s, presumably due to field-induced renormalization of the c -axis dispersion (due to Landau quantization, see below). The lower panel of Fig. 1 shows the in-plane resistivity $\rho(T)$ for B applied along an in-plane direction. Note how T_{co} as well as the low T resistivity is markedly suppressed by $B > 20$ T applied along the CoO_2 planes. The suppression of a CO-state by an external field is not surprising since it has been shown that a charge-density wave (CDW) can be destabilized by an external field surpassing the Pauli limit [11, 12]. In our case, the anisotropy of the Pauli critical field could be attributed to

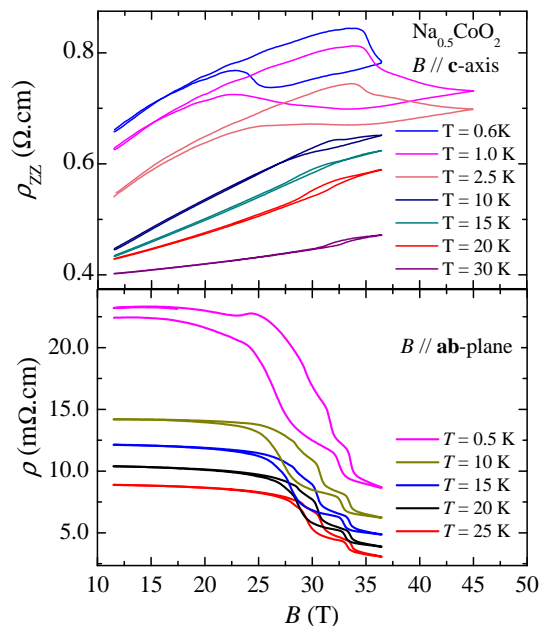


FIG. 2: Upper panel: Inter-plane resistivity ρ_{zz} as a function of magnetic field B for a $\text{Na}_{0.5}\text{CoO}_2$ single crystal and for several values of temperature. Lower Panel: In-plane resistivity ρ as a function of B applied along the planes, for a second $\text{Na}_{0.5}\text{CoO}_2$ single crystal and for several values of T . Notice the sharp decrease of ρ for $B > 25$ T.

the anisotropy of the Landé g factor [13], since the susceptibility is highly anisotropic. By analogy to superconductors, the Pauli critical field in a one-dimensional CDW is estimated to be $B_P = \Delta_0 / (\sqrt{2}gS\mu_B)$. [12] The optical gap has been measured to be 13.64 meV or 158 K. [14] Interpreting this as $2\Delta_0$, and assuming $g = 2$, $S = \frac{1}{2}$, we estimate $B_P \approx 83$ T. This is somewhat larger than the observed field of 40 T, but not unreasonable given the uncertainty concerning g and Δ_0 and the applicability of the one dimensional model.

Figure 2 shows both ρ_{zz} as a function of $B \parallel c$ -axis (upper panel) as well as ρ as a function of $B \perp c$ -axis (lower panel) for several values of the temperature T . Notice how inter-plane fields in excess of 25 T have a modest but quite hysteretic effect on ρ_{zz} , suggesting a partial destabilization of the CO-state. By contrast, fields applied along the conducting planes lead to a significant (factor of 3) reduction in ρ . The effect of B is clearly far more pronounced for in-plane fields. The steps seen in ρ at higher B could correspond to metastable configurations of the CO state. The most significant feature of the ρ_{zz} data is undoubtedly the appearance of SdH oscillations at low T as seen in the upper panel of Fig. 2. The top panel in Fig. 3 shows an example of the isolated SdH signal defined as $(\sigma - \sigma_b) / \sigma_b$, where σ is the inverse of ρ_{zz} and σ_b is the inverse of the background resistivity as a function of inverse field B^{-1} at $T = 0.6$

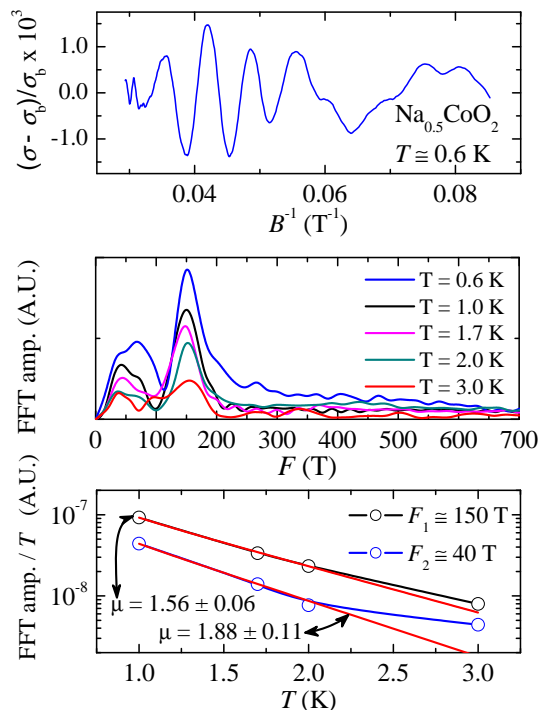


FIG. 3: Upper panel: The Shubnikov de Hass signal, defined as $(\sigma - \sigma_b)/\sigma_b$, where $\sigma = 1/\rho_{zz}$ and $\sigma_b = 1/\rho_b$ with ρ_b being the background resistance, as a function of the inverse of the magnetic field B^{-1} . Middle panel: The FFT of the SdH signal for several temperatures. Two peaks are observed at $F_1 \simeq 150$ T and $F_2 \simeq 40$ T, respectively. Lower panel: The amplitude of both peaks in the FFT signal, normalized respect to the temperature T , and as a function of T . Red lines are fits to the Lifshitz-Kosevich expression $x/\sinh x$, from which we extract the effective masses μ .

K. Note that only a few oscillations are observed over a broad range of B . The middle panel of Fig. 3 shows the amplitude of the FFT signal as a function of the SdH frequency F for several values of T . A main peak with $F_1 \simeq 150$ T is clearly observed in the temperature evolution of the FFT signal with a second weaker peak appearing at $F_2 \simeq 40$ T. Using the Onsager relation $F = A(hc/4\pi^2e)$, where A is the FS cross-sectional area perpendicular to B , and the orthorhombic lattice parameters reported in Ref. [5], these frequencies correspond to pockets with cross-sectional areas occupying only 1 and .25% of the area of the orthorhombic Brillouin zone, respectively. Note that this is only 0.25 and 0.0625% of the undistorted hexagonal Brillouin zone. Of course SdH only tells us the area of each pocket and not the number of pockets. Nevertheless, a change of Fermi surface topology and a dramatic reduction in the carrier density is consistent with Hall measurements which show a sign change at the transition temperature and an increase of the magnitude of R_H by a factor of 250. [3]. For $B \parallel c$ -axis no SdH oscillations were observed in the

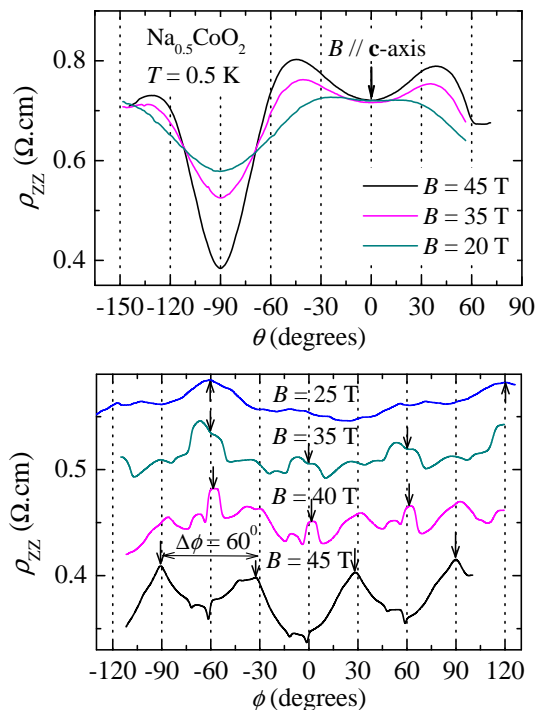


FIG. 4: Upper panel: Inter-plane resistivity ρ_{zz} as a function of the angle θ between the external magnetic field B and the inter-plane c -axis and for several values of the external field. The pronounced drop in ρ for $B \parallel a$ - b plane is due to the partial suppression of the CO-state at this orientation. Lower panel: Angular magnetoresistance oscillations for field applied along the conducting planes. Notice how the nearly two-fold symmetric behavior progressively disappears in favor of a 6-fold one as the CO state is suppressed.

hysteretic region, probably due to the absence of a well defined coherent FS around the transition.

In the Lifshitz-Kosevich [15] (LK) formalism, the ratio of each harmonic p of the oscillatory component of the conductivity $\tilde{\sigma} = (\sigma - \sigma_b)$ to the monotonically varying background σ_b has the form:

$$\frac{\tilde{\sigma}}{\sigma_b} \propto \frac{(-1)^p}{p^{3/2}} R_{T,p} R_{D,p} R_{s,p} \left[2\pi p \left(\frac{F}{B} - \gamma \right) \pm \frac{\pi}{4} \right] \quad (1)$$

where $R_{T,p} = (\alpha p \mu T / B) / \sinh(\alpha p \mu T / B)$, $R_{D,p} = \exp[-\alpha p \mu T_D / B]$ and $R_{s,p}$ are the temperature, Dingle and spin damping factors, respectively [15]. In the above expressions $\alpha = 2\pi^2 k_B m_e / e \hbar$, μ is the quasiparticle's effective cyclotron mass in relative units of the free electron mass m_e , and T_D is the so-called Dingle temperature $T_D = \hbar / 2\pi k_B \tau$ that provides an accurate value for the quasiparticles relaxation time τ . Thus, in order to obtain the effective masses μ for both orbits F_1 and F_2 we plot in the lower panel of Fig. 3 the amplitude of the FFT signal normalized respect to the temperature T . The red lines are fits to the temperature damping factor $R_{T,p}$ from which we obtain $\mu_1 = 1.6 \pm 0.1$ for F_1 and $\mu_2 = 1.9 \pm 0.1$

for F_2 , respectively. These effective masses are light if we recall that an effective mass of order $70 m_e$ was extracted for $x = 0.6$ and $x = 0.7$ from ARPES and in specific heat measurements. The light mass however is quantitatively consistent with the reduction of the Sommerfeld coefficient for $x = 0.5$, obtained by extrapolating the heat capacity C/T to $T = 0$ [5]. This is an important point since it indicates the absence of additional Fermi surfaces of heavier masses that might not have been detected in the present study. Finally, in order to estimate the quality of our samples, we performed a semi-logarithmic Dingle plot, obtaining the surprisingly low value $T_D \simeq 3.3 \pm 0.5$ K. From T_D we obtain $\tau = (3 \pm 0.5) \times 10^{-13}$ s, corresponding to $\omega_c \tau \simeq 0.85 \pm 0.13$ at 25 T and a mean free path $l = v_F \tau = \hbar(A/\pi)^{1/2} \tau / \mu \sim 145$ Å. This implies $k_F l = 9.7$ where $k_F = (A/\pi)^{1/2}$ is the radius of the pockets. Thus the observation of SdH oscillations indicate that the crystal is sufficiently clean and that the residual Fermi pocket should be metallic. However, from Fig. 1, lower panel, we see that the resistivity is insulating-like, due to the loss of charge carriers when the gap opens. One explanation is that the bulk resistivity is not intrinsic, but dominated by scattering from CDW domain boundaries in some complicated way. Alternatively, the SdH signal may originate from a small part of the sample where the Na is particularly well ordered.

Angular magnetoresistance oscillations have been proven to be a powerful way of extracting the 3D geometry of the FS in overdoped cuprates [16]. We are currently applying these techniques to Na_xCoO_2 and the current results obtained for $x = 0.5$ are displayed in Fig. 4 which shows the dependence of the inter-plane magnetoresistance ρ_{zz} on the angle θ between B and the inter-plane c -axis, at $T = 0.6$ K and for several values of B . A pronounced dip is observed when the field is aligned along the in-plane direction, due to the destabilization of the CO-state. Two peaks are observed at $\pm 45^\circ$ that are most likely associated with genuine Yamaji effects whose angular position depends on both the FS size and the complexity of the c -axis dispersion [16]. The lower panel of Fig. 4 shows ρ_{zz} as a function of the azimuthal angle ϕ between B and an in-plane axis. At lower fields, $\rho_{zz}(\phi)$ is essentially two-fold, with some small poorly defined structures at intermediate angles. Notice that this structure cannot result from a cylindrical FS of circular cross-section, since k_F , v_F and τ would remain uniform across its perimeter and consequently $\rho_{zz}(\phi)$ would remain constant. The observed two-fold periodicity reflects, in fact, the symmetry of the orthorhombic structure resulting from the Na ordering. A similar effect was reported in the tetragonal $\text{Tl}_2\text{Ba}_2\text{CuO}_6$ compound [17], where $\rho_{zz}(\phi)$ displays a 4-fold periodicity due to the 4-fold modulation induced on k_F , v_F , and τ by the structure of the CuO_2 planes. In our case, the two-fold dependence of $\rho_{zz}(\phi)$ progressively disappears as B increases (with the emergence, at the CO to metallic transition,

of field dependent fine structures) and stabilizes into a 6-fold one at higher fields. This periodicity is consistent with both the triangular symmetry of the CoO_2 planes and with the hexagonal FS measured by ARPES [6]. It is remarkable that once the CO state is suppressed, the resulting metallic state seems oblivious to the Na order.

In summary, we have presented a detailed electrical transport study on $\text{Na}_{0.5}\text{CoO}_2$, observing both Shubnikov-de Haas oscillations and two-fold angular magnetoresistance oscillations in its charge-ordered state. Both the frequency of the SdH oscillations and the periodicity of the in-plane AMRO at low fields indicate that the Na ordering introduces profound effects on the electronic structure of this compound. Moreover, a relatively modest in-plane magnetic fields is found to suppress the charge ordered gap leading to a correlated metal. At high fields, an in-plane AMRO displaying a 6-fold modulation emerges. These facts indicate that the charge order is a delicate one, more akin to a CDW, and consistent with the small optical gap.[14] Clearly, the interplay between Na ordering and charge ordering in these strongly correlated materials remains a challenging problem.

This work was performed at the NHMFL which is supported by NSF through NSF-DMR-0084173, the State of Florida and DOE. One of us (LB) acknowledges support from the NHMFL in-house research program. FCC acknowledges support from the MR-SEC Program of the National Science Foundation under award number DMR-02-13282 and from DOE under grant number DE-FG02-04ER46134. PAL acknowledges NSF award number DMR-0201069.

-
- [1] K. Takada *et al.*, Nature (London) **422**, 53 (2003); R. Schaak *et al.*, *ibid* **424**, 527 (2003).
 - [2] M. L. Foo *et al.*, Solid State Commun. **127**, 33 (2003); J. Lynn *et al.*, Phys. Rev. B **68**, 214516 (2003).
 - [3] M. L. Foo *et al.*, Phys. Rev. Lett. **92**, 247001 (2004).
 - [4] H. W. Zandbergen *et al.*, Phys. Rev. B **70** 024101 (2004).
 - [5] Q. Huang *et al.*, cond-mat/0402255 (2004); cond-mat/0406570 (2004).
 - [6] M. Z. Hasan *et al.*, Phys. Rev. Lett. **92**, 246402 (2004); H. -B. Yang *et al.*, *ibid* **92**, 246403 (2004)
 - [7] D. J. Singh, Phys. Rev. B **61**, 13397 (2000)
 - [8] K. -W. Lee, J. Kunes, and W. E. Pickett, Phys. Rev. B **70**, 045104 (2004).
 - [9] M. D. Johannes, I. I. Mazin, D. J. Singh, and D. A. Papaconstantopoulos, Phys. Rev. Lett. **93**, 097005 (2004).
 - [10] F. C. Chou *et al.*, J. Phys. Chem. Sol. (to be published); F. C. Chou *et al.*, Phys. Rev. Lett. **92**, 157004 (2004).
 - [11] D. Graf *et al.*, Phys. Rev. B **69**, 125113 (2004).
 - [12] R. D. McDonald *et al.*, Phys. Rev. Lett. **93**, 076405 (2004).
 - [13] F. C. Chou, J. H. Cho, and Y. S. Lee, Phys. Rev. B (to be published).
 - [14] J. Hwang, J. Yang, T. Timusk, and F.C. Chou, cond-mat/0405200.

- [15] See for instance, *D. Shoenberg, Magnetic Oscillations in Metals* (Cambridge University Press, Cambridge, England, 1984) and references therein.
- [16] N. E. Hussey *et al*, *Nature* **425**, 814 (2003).
- [17] N. E. Hussey *et al.*, *Phys. Rev. Lett.* **76**, 122 (1996), and references therein.